

In Vivo Confocal Endomicroscopy of Small Intestinal Mucosal Morphology in Dogs

M.J. Sharman, B. Bacci, T. Whittam, and C.S. Mansfield

Background: Confocal endomicroscopy (CEM) is an endoscopic technology that permits in vivo cellular and subcellular imaging of the gastrointestinal mucosa.

Objective: To determine the feasibility of CEM to evaluate small intestinal mucosal topologic morphology in dogs and to characterize the appearance in healthy dogs.

Animals: Fourteen clinically healthy research colony dogs.

Methods: Experimental study. Dogs were anesthetized for standard endoscopic evaluation of the small intestine followed by CEM. Two fluorophores were used to provide contrast: fluorescein (10% solution, 15 mg/kg IV) before administration of topical acriflavine (0.05% solution) via an endoscopy spray catheter. A minimum of 5 sites within the small intestine were assessed and at each location, sequential adjustment of imaging depth allowed collection of a three-dimensional volume equivalent to an 'optical biopsy'. CEM-guided pinch biopsies were obtained for histologic examination.

Results: CEM provided high-quality in vivo cellular and subcellular images. Intravenous administration of fluorescein provided sufficient contrast to allow assessment of the vasculature, cellular cytoplasmic features and goblet cell numbers, and distribution. Topical application of acriflavine preferentially stained cellular nucleic acids, allowing evaluation of nuclear morphology. Quality of captured images was occasionally affected by motion artifact, but improved with operator experience.

Conclusion and Clinical Importance: CEM provides in vivo images that allow for cellular and subcellular assessment of intestinal mucosal morphology during endoscopy. This has implications for aiding in vivo diagnosis of gastrointestinal disease.

Key words: Acriflavine; Endoscopy; Fluorescein; Gastroenterology; Gastrointestinal.

Confocal endomicroscopy (CEM) permits simultaneous wide-field, white light endoscopy (WLE), and real-time, microscopic imaging of the gastrointestinal mucosa.^{1–4} This is achieved either by integration of a miniaturized confocal microscope into a conventional flexible endoscope, or by the use of confocal mini-probes passed through the biopsy channel of a conventional video-endoscope.^{1,4} Intravenous or topical administration of exogenous fluorophores provides fluorescent contrast to produce an image equivalent to 1000× magnification.^{1,5,6} Histologically equivalent 'virtual biopsies' can, therefore, be obtained.^{7,8}

The ability to perform real-time evaluation of topologic mucosal morphology potentially provides in vivo diagnostic capability.^{8,9} In people, CEM is used for clinical assessment of a range of gastrointestinal disorders encompassing dysplastic, neoplastic, inflammatory, and auto-immune disease.^{1,3,8,10–13} Evaluation of CEM in diseases of importance to companion animal medicine is limited.

From the Faculty of Veterinary Science, The University of Melbourne, Melbourne, Vic, Australia (Sharman, Bacci, Whittam, Mansfield). This study was presented at the 2013 American College of Veterinary Internal Medicine Forum, Seattle, Washington. This study was performed at The University of Melbourne, Victoria, Australia.

Corresponding authors: M.J. Sharman and C.S. Mansfield, Faculty of Veterinary Science, The University of Melbourne, 250 Princes Highway, Werribee, Vic 3030; e-mail: melloras@unimelb.edu.au or cmans@unimelb.edu.au.

Submitted May 3, 2013; Revised July 3, 2013; Accepted September 3, 2013.

Copyright © 2013 by the American College of Veterinary Internal Medicine

10.1111/jvim.12214

Abbreviations:

CEM	confocal endomicroscopy
FITC	fluorescein isothiocyanate
RBCs	red blood cells
WLE	white light endoscopy
WSAVA	World Small Animal Veterinary Association

The aims of this study were to evaluate the feasibility of CEM using administration of topical and intravenous exogenous fluorophores to evaluate and describe normal small intestinal mucosal epithelial and vascular topographic morphology in dogs.

Materials and Methods

Animals

Fourteen healthy adult mix-breed research colony dogs (10M, 4F) were studied. Dogs were housed within the University of Melbourne's dog colony; and were considered healthy based on a combination of physical examination, routine hematology, and serum biochemistry prior to inclusion. Vaccinations and parasite prophylaxis were current for all dogs. The University of Melbourne's Animal Ethics Committee approved all dog use according to National Health and Medical Research Council guidelines (Institutional Animal Care and Use Committee Approval numbers 1112209 and 1112075).

Equipment

Endoscopic procedures were performed using one of two prototype confocal endomicroscopes developed by integration of a miniaturized confocal microscope into a standard video-endoscope (Olympus, GIF-Q145 and Olympus PCF-Q180A1).^{ab} For confocal imaging, a solid-state laser with a variable power output

(0–1000 μ W) delivered 488 nm (blue) laser light via a single optical fiber capable of focusing to a single, diffraction limited, plane within the tissue. Fluorescence in the range of 405–590 nm wavelengths was detectable. Image depth could be varied up to 250 μ m, at \sim 3 μ m increments with acquisition of images throughout this depth range (z -axis). This allowed sampling of a three-dimensional volume equivalent to an ‘optical biopsy’. Axial (7 μ m) and lateral (0.5 μ m) resolution permitted evaluation of both cellular and subcellular detail.

Procedure

Dogs were fasted for 12 hours before gastroduodenoscopy. Each dog received sedation with acepromazine (0.01 mg/kg IV)^c and methadone (0.1 mg/kg IV)^d prior to induction of anesthesia with alfaxalone (2 mg/kg IV).^e General anesthesia was maintained with isoflurane^f in oxygen and all dogs received supportive fluid therapy IV for the duration of the procedure (Hartmann’s solution, 10 mL/kg/h).

After gross morphologic assessment of the duodenum using standard WLE, fluorescein (15 mg/kg; 10% aqueous solution)^g was administered IV as a bolus via the peripheral fluid line as previously described.⁶ Confocal endomicroscopy was performed concurrently with video-gastroduodenoscopy by placing the tip of the endoscope containing the confocal microscope in direct contact with, and *en face* to the mucosal surface. Gentle suction was applied, where necessary, to stabilize the image for acquisition and interpretation. A minimum of 5 sites at various and random depths of insertion of the endoscope within the small intestine were assessed. At each location, ‘optical biopsies’ were obtained by sequentially adjusting the z -axis by \sim 6–9 μ m intervals until resolution and contrast was insufficient for adequate image interpretation. Images were obtained at a variety of frame rates and resolutions ranging from 0.8 frames/s at 2.1 megapixels to 6 frames/s at 0.25 megapixels.

Once assessment with fluorescein was complete, acriflavine (20–50 mL of 0.05% aqueous solution)^g was applied topically to the duodenal mucosal surface via an endoscopy spray catheter (Olympus washing catheter (PW-2L-1)).^a A further 5 sites were then randomly chosen and evaluated. In 1 dog, Cresyl Violet (40 mL of 0.25% aqueous solution)^g was additionally assessed in a region separate to that where acriflavine had been applied.

Multiple endoscopic pinch biopsy specimens (6–10 per dog) were collected from corresponding regions of the duodenum and preserved in 10% buffered formalin. Serial sections (4–5 μ m) of paraffin-embedded samples were obtained and stained with hematoxylin and eosin (H&E). Samples were positioned as for standard histologic assessment, but were also positioned orthogonal to this, *en face* to the mucosal surface, to correspond with some of the confocal images. Confocal images were evaluated and described in combination with corresponding histopathologic images, by two authors (BB and MJS). Histologic standards for the diagnosis of gastrointestinal inflammation, developed by the World Small Animal Veterinary Association (WSAVA) Gastrointestinal Standardization Group, were used to interpret histologic sections.¹⁴

The presence and frequency of CEM image artifacts that interfered with confocal image interpretation was assessed by review of all captured images from each of the first 6 procedures, all of which had been performed by a single user. Procedures were reviewed in a random order by 2 authors (MJS and CSM) and the number of images affected by each artifact was expressed as a percentage of the overall number of images captured. Image artifact included, but was not limited to, poor mucosal contact, imaging interference attributable to luminal debris and motion artifact.

Results

Gross mucosal abnormalities were not detected within the regions examined via WLE in any of the dogs. CEM evaluation of the duodenal mucosa was easily performed using the technique described and all three agents evaluated allowed sufficient fluorescent contrast for image acquisition and interpretation. Fluorescein was redistributed from the vascular space to the interstitial and intracellular spaces within seconds of intravenous administration and fluorescent contrast was adequate for imaging for a minimum duration of 30 minutes in all dogs evaluated. For topical agents, fluorescence was limited to the region of application, requiring reapplication for each new area assessed.

On contact with the mucosa, intestinal villi were visualized as finger-like projections extending from the surface and were mostly seen in longitudinal, rather than transverse section. Shallow invaginations, extending regularly across the surface of each villi, were identified (Fig 1B, D, and F) and the epithelial cell brush border was highlighted along these folds, with each fluorophore. Depending upon the particular fluorescent contrast agent used, the microvascular network and various cell types, including mucin-containing goblet cells, columnar epithelial cells, and cells within the lamina propria could be differentiated based on their staining characteristics.

By adjustment of the z -axis, imaging with fluorescein was useful to a depth of approximately 80–120 μ m at which point resolution became insufficient to allow accurate interpretation of cellular detail. With either of the topical fluorophores, useful imaging to a depth of approximately 50–70 μ m was possible. As operator experience and confidence improved, an overview of a particular region was more frequently gained by increasing the rate of scanning to allow quick assessment of a larger section of the mucosal surface. Although these images were of lower resolution, they still allowed evaluation of gross mucosal morphology including blood flow. Representative CEM images from each of the agents assessed along with corresponding standard histopathologic images are provided in Figure 1A–F.

Fluorescein

Fluorescein allowed evaluation of the vasculature and cellular cytoplasmic features (Fig 1B and C). Nuclear contents were not stained and therefore nuclear characteristics could not be evaluated. Based on histologic correlates, goblet cells showed a recognizable shape and position and were seen as scattered, polarized cells with a dark cytoplasmic vacuole within the apical portion. In cross-section, this resulted in a characteristic target staining pattern. Fluorescence of goblet cells was reduced in comparison to adjacent epithelial cells and assessment of both the numbers and distribution of goblet cells was possible.

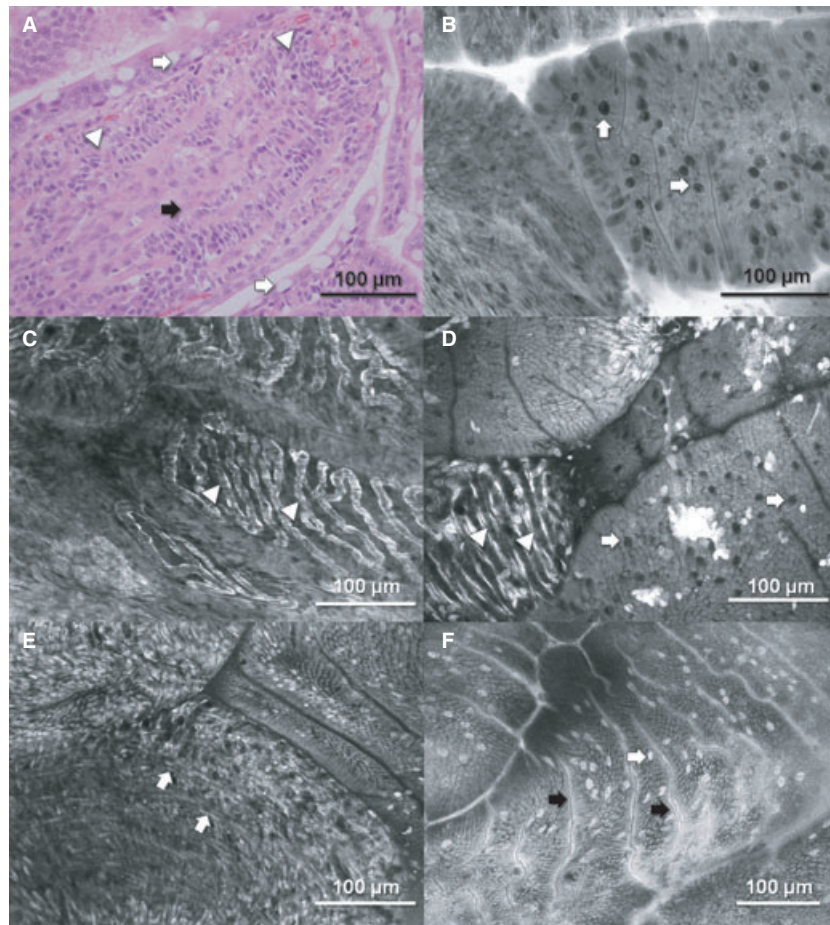


Fig 1. (A) Standard histopathologic image of the duodenum H&E. Comparative histopathologic image of the duodenal villi in longitudinal section showing goblet cells within the superficial epithelial layer (white arrows), the smooth muscle within the lamina propria (black arrow), and what can be seen of the microvascular network (white arrow heads). (B, C) **Fluorescein Images.** Confocal endomicroscopy (CEM) image of the tips of the duodenal villi. Intravenous administration of fluorescein highlights cellular cytoplasmic features, but not nuclear detail. Superficial imaging of the villi demonstrates numbers and distribution of goblet cells (arrows) and shallow invaginations extending regularly across the surface are also identified. C. Within deeper cross-sections, the uniform arrangement of the columnar epithelial cells along the basement membrane can be delineated along with the dense, subsurface microvascular network (white arrow heads). (D, E) **Acriflavine Images.** Administration of topical acriflavine results in preferential staining of nuclear contents allowing improved visualization of individual cells. With superficial imaging, the regular pattern of the mucosal epithelial cells can be seen, interspersed with characteristic goblet cells (arrows). Deeper sections show the nuclei of cells within the lamina propria and extending longitudinally through the core are fine linear structures, correlating with strands of smooth muscle from the muscularis mucosae. Vascular detail was occasionally visualized negatively contrasting against the positive background of the lamina propria and highlighted by staining of the endothelial cell nuclei (arrow heads). (F) **Cresyl Violet.** Cresyl violet distributed to both the cytoplasm and nucleus and compared with both fluorescein and acriflavine, goblet cells showed intense fluorescence (white arrow). Ultrastructural detail such as the epithelial brush border was distinguishable (black arrows).

By adjusting the focal plane, the uniform arrangement of the columnar epithelial cells along the basement membrane could be delineated along with the dense, subsurface microvascular network within the lamina propria at the core of each intestinal villi (Fig 1C). Red blood cells (RBCs) were not labeled and were, therefore, seen as round, negatively staining, silhouettes within the vascular space and their movement could be tracked real-time, especially at faster scan speeds. Vascular congestion was occasionally noted as stacking of RBCs at focal points along the length of the vessel, or where congestion was more extensive, as vessels negatively contrasting against the positive

fluorescence of the lamina propria (Fig 2B). This was often associated with excessive application of pressure or suction for image acquisition and blood flow was restored by reducing these factors.

Acriflavine

Topical application of acriflavine resulted in preferential nuclear staining, allowing visualization of individual cells within both the epithelial surface layer and the lamina propria (Fig 1D and E). Cytoplasmic and subcellular detail was also superior to acriflavine compared with fluorescein. With superficial imaging,

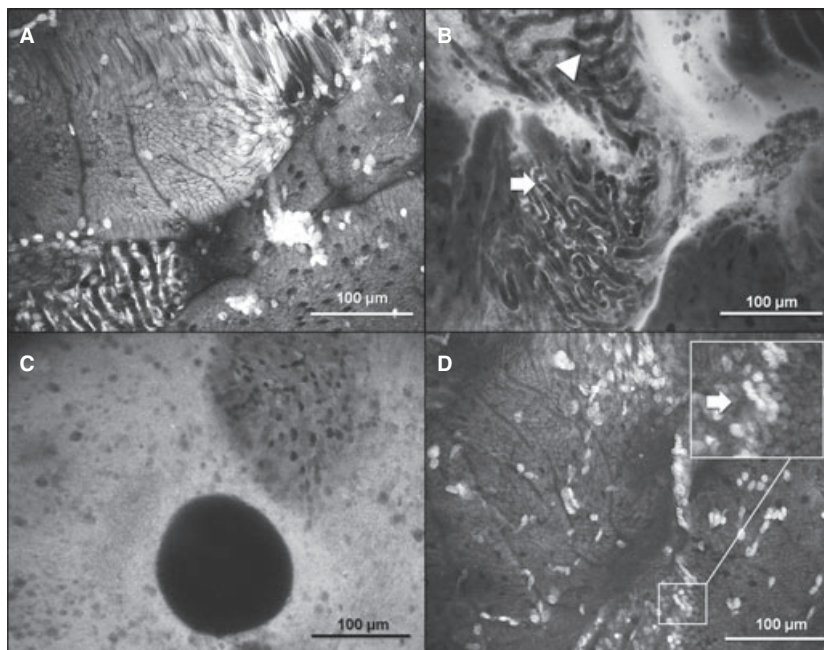


Fig 2. (A–D) Imaging Artifacts. (A) **Motion artifact.** Confocal endomicroscopy image collected after topical administration of acriflavine. Note that the top of the image is affected by motion, but the remainder of the image is of good quality. (B) **Vascular congestion.** Vascular congestion of the microvascular network observed as both stacking of red blood cells along the length of the vessel (arrow) as well as negatively contrasting microvasculature against the positive fluorescence of the lamina propria (arrow head). Image collected after intravenous administration of fluorescein. (C) **Poor mucosal contact and gas-bubble artifact.** A complete image, as seen in the other images, is not observed and a large, negatively contrasting, circular artifact consistent with a gas-bubble, obscures the lower image. Image collected after intravenous administration of fluorescein. (D) **Cellular Debris and Vibrational artifact.** Cellular debris can be seen in the foreground of this image taken after topical administration of acriflavine. Subtle vibration of the optical fiber is also present obscuring the width of the lower image (magnified image inset).

mucosal epithelial cells formed a regular pattern over the surface of intestinal villi, interspersed with characteristic goblet cells. Within deeper sections of intestinal villi, nuclei of the superficial columnar epithelial cells could be visualized lining up against the basement membrane and individual lamina propria cells were identifiable. Vascular detail was not always appreciated, but occasionally, the dense microvascular network was visualized negatively contrasting against the positive background of the lamina propria and highlighted by positive staining of the endothelial cell nuclei by acriflavine (Fig 1D).

Extending longitudinally through the core of the intestinal villi, fine linear structures were observed (Fig 1E). Based on histologic correlates, these corresponded to strands of smooth muscle. Lymphatics were not easily differentiated.

Cresyl Violet

In the 1 dog assessed, cresyl violet was distributed to both the cytoplasm and nucleus (Fig 1F). Goblet cells showed their characteristic target pattern, as seen with both fluorescein and acriflavine; however, fluorescence was much more intense in comparison to that seen with either of the other fluorophores. Ultrastructural detail such as the epithelial brush border was also distinguishable. Distribution, uptake, and fluorescent intensity

improved with dwell time, but were frequently uneven across the field of view being evaluated.

Histopathology

Standard histopathologic examination of duodenal endoscopic biopsies identified mild-to-moderate lymphoplasmacytic infiltrates in 13/14 dogs according to WSAVA guidelines.^{14,15} This was superficial, remaining only within the villous tips in 12 and extending into the crypts in 1. Mild hyperemia was noted in 3 dogs, and was suspected to be secondary to the use of suction during CEM imaging. In 1 dog, occasional focal accumulations of neutrophils were additionally noted, along with an increased number of intraepithelial lymphocytes.

Review of small intestinal CEM images in this dog showed no appreciable differences in villous morphology including cellularity of the lamina propria or changes within the epithelial border compared with the other dogs.

Image Artifacts

A total of 2464 CEM images of the small intestinal mucosa were collected during the first 6 procedures and were assessed for the presence of artifacts. These procedures were chosen for further evaluation as each had been performed by a single user, whereas the

subsequent 8 procedures were performed by a combination of users. Motion secondary to peristalsis was the most common CEM imaging artifact (Fig 2A) being observed in 504 of 2464 (20.4%) images. Other imaging artifacts included uneven contact with the mucosal surface, resulting in incomplete images, and rarely gas bubbles and vibration of the optical fiber (Fig 2A–D). Artifacts resulting from poor mucosal contact were resolved either by applying suction, or by breaking and re-establishing contact with the mucosal surface. Luminal debris and epithelial shedding from the villous surface also intermittently obscured imaging or contributed to poor mucosal contact. When adhered to the confocal window, debris contributed to decreased image resolution when the *z*-axis was adjusted to a deeper focal plane. This was generally resolved by wiping the distal tip of the endoscope containing the confocal window gently across the mucosal surface.

With increasing operator experience, both the total number of images acquired during a study and the percentage affected by imaging artifact decreased appreciably. The main CEM operator in this study (MJS) captured an average of 350 images/procedure across 5 procedures, with motion artifact affecting 92/427 images (21.0%) in procedure 1, compared with 4/260 images (1.5%) in their 5th procedure. When an operator with no prior experience of CEM performed procedure 5 in the series of 6 reported, the number of images captured increased substantially to 710. The number of captured images affected by motion artifact also increased to 290/710 (40.8%) compared with 15/326 (4.6%) in procedure 4, which was performed by the more experienced operator.

Discussion

This study demonstrates that instantaneous acquisition of histologic-equivalent images of the canine small intestinal mucosa using CEM is feasible during endoscopy, using the fluorophore protocols described. All 3 fluorophores used in this study provided adequate fluorescent contrast and allowed for both an overall impression of gross intestinal villous morphology and detail regarding vascular, cellular, and subcellular features. Morphologic features identified via CEM were comparable to standard histologic correlates.

Each fluorophore evaluated demonstrated unique fluorescent characteristics and therefore provided complementary information regarding components of mucosal morphology. Intravenous administration of fluorescein proved superior for evaluating the microvascular network, including blood flow, but still allowed evaluation of the columnar epithelial layer, the extracellular matrix of the lamina propria and goblet cell numbers and distribution. In comparison, the administration of topical agents acriflavine and cresyl violet provided superior nuclear detail allowing improved identification of individual cells. In addition, intravenous administration of fluorescein resulted in distribution throughout the entire assessable depth of the

intestinal mucosa while topical fluorophores had more limited penetration.

Both fluorescein and acriflavine have been routinely used clinically in people. However, safety concerns regarding the potential mutagenic effects of acriflavine, because of its preferential staining of nucleic acids, have led to fluorescein gaining more routine use for gastrointestinal CEM.^{1,4,16} These fluorophores have similar excitation and emission characteristics that match equipment specifications.^{5,17,18}

Cresyl violet has received more limited assessment in conjunction with CEM, requires higher laser power to provide sufficient fluorescent contrast, and appears less reliable.⁵ Similar results were achieved in our study. Both the excitation and emission wavelength specifications of the CEM system being used were at the limits for cresyl violet and this likely contributed to the poor utility of cresyl violet in this study.⁵ Unpredictable uptake and precipitation at the mucosal surface also limit its routine clinical use.

In people, the use of CEM has identified increased lamina propria cellularity, nuclear aberrations or characteristic changes in gastric or colonic pit, and vascular patterns that correspond with inflammation, infiltrative neoplasia, or neoplastic transformation.^{12,19–21} In autoimmune and inflammatory gastrointestinal disorders, CEM has also documented bacterial translocation, increased epithelial shedding, and alterations in epithelial and vascular permeability.^{22–26} By conjugation of fluorescein isothiocyanate (FITC) with different molecular weight dextrans, retention within the vascular space can be increased, and more subtle alteration in vascular permeability can be assessed in vivo using confocal imaging.^{27,28} Specific targeting and identification of individual leukocytes could also be achieved using fluorescently labeled antibodies in airways.²⁹ For some of these changes, ex vivo evaluation is impossible or prone to processing artifact. Furthermore, although standard histopathology is limited by the number of adequate endoscopic biopsies collected, CEM can be used to assess both a greater region and number of sites within the mucosa, and potentially target mucosal abnormalities for biopsy when lesions are detected.

Based on this study, similar potential exists for disease detection in dogs. In the case with identifiable histopathologic changes seen in this series, no appreciable difference was noted on evaluation of the confocal images compared with the other dogs. This may be because change within the intestinal mucosa was too subtle to be identified with CEM. Alternatively, further evaluation and more experience interpreting CEM images in combination with histopathology may allow such subtle differences to be appreciated. In this study, imaging depth was limited to a maximum of 120 μ m despite the ability to vary depth up to a 250 μ m. This has the potential to limit interpretation in diseases where submucosal involvement is important for definitive diagnosis. Whether or not this proves a real limitation in disease remains to be determined as alternate superficial mucosal features could be detectable that equally correspond with submucosal lesions

as determined by more traditional methods. This could include subtle alteration to mucosal morphology or to the microvascular network, such as changes in blood flow and vascular permeability, or both. Further evolution of the technology over time or adaptation to encompass infrared laser light could also improve axial resolution and therefore aid deeper imaging.

Correct interpretation of CEM images requires some investigator experience and specific training, using images with confirmed histopathologic diagnoses, has been shown to be useful to rapidly improve *in vivo* detection of disease.^{9,30–32} As demonstrated here, the technique of operating the CEM and obtaining usable confocal images also entails a steep learning curve that improves with increasing operator experience.³¹ In this study, both the number of captured images and the percentage affected by artifact reduce as operator experience increased. As operator confidence improved, an overview of a whole region was more frequently gained by increasing the rate of scanning to cover a larger section of the mucosal surface. Although these images were of lower resolution, this method could still be useful to detect mucosal abnormalities, at which point scan rate can be decreased again for image capture at the highest resolution.

Image artifacts were easily recognized real-time during positioning and could be avoided or corrected where necessary during the process of image acquisition. In addition, artifacts were often trivial and did not preclude wider assessment of the captured image in the majority of cases. Whether or not some of these imaging artifacts, such as the degree of cellular debris or microvascular congestion, might be induced by the exogenous fluorophore protocols used or by irritation from, the endoscope itself is difficult to absolutely determine. However, as artifacts usually affected only isolated regions of the mucosa, and often were identified on first contact with the mucosa, this is considered unlikely. With additional experience, as well as with further evaluation of alternate fluorophore protocols, this might be able to be determined.

In conclusion, CEM provides *in vivo* histologically equivalent images, allowing assessment of mucosal topologic morphology during endoscopy in dogs. This has implications for aiding *in vivo* diagnosis of gastrointestinal conditions; however, further assessment in a larger number of dogs with disease is required.

Footnotes

^a Olympus Australia, Mt Waverley, Vic, Australia

^b Optiscan Imaging, Notting Hill, Vic, Australia

^c ACP 2 Delvet Pty Ltd, Asquith, NSW, Australia

^d Physeptone; Sigma Pharmaceuticals, Rowville, Vic, Australia

^e Alfaxan; Jurox Pty Ltd, Rutherford, NSW, Australia

^f Isorrane; Baxter Healthcare Pty Ltd, Old Toongabbie, NSW, Australia

^g Sigma Aldrich, Castle Hill, NSW, Australia

Acknowledgments

The authors thank Peter Delaney from Optiscan Imaging for assistance with the initial confocal endomicroscopy procedures; and Dr Julien Dandrieux, Dr Nathalee Prakash, and Dr Anne-Claire Duchaussoy for additional procedural assistance.

The study was supported, in part, by grants from the Comparative Gastroenterology Society Waltham's Research grant and by the Victorian Government's Operational Infrastructure Support Program. The confocal endomicroscope was purchased by the University of Melbourne and the Victorian Department of Business and Innovation; Victorian Science Agenda. This equipment forms part of the Victorian Biomedical Imaging Capability.

Conflict of Interest: Dr Mellora Sharman and Dr Ted Whittem own minor stock in Optiscan Imaging.

References

- Dunbar KB, Canto MI. Confocal endomicroscopy. *Tech Gastrointest Endosc* 2010;12:90–99.
- Goetz M, Dunbar K, Canto M. Examination technique of confocal laser endomicroscopy. In: Kiesslich R, Galle PR, Neurath MF, eds. *Atlas of Endomicroscopy*. Heidelberg: Springer; 2008:25–32.
- Kiesslich R, Goetz M, Neurath MF. Confocal laser endomicroscopy for gastrointestinal diseases. *Gastrointest Endosc Clin N Am* 2008;18:451–466.
- Kiesslich R, Goetz M, Vieth M, et al. Confocal laser endomicroscopy. *Gastrointest Endosc Clin N Am* 2005;15:715–731.
- Goetz M, Toermer T, Vieth M, et al. Simultaneous confocal laser endomicroscopy and chromoendoscopy with topical cresyl violet. *Gastrointest Endosc* 2009;70:959–968.
- Sharman M, Mansfield C, Whittem T. The exogenous fluorophore, fluorescein, enables *in vivo* assessment of the gastrointestinal mucosa via confocal endomicroscopy: Optimization of intravenous dosing in the dog model. *J Vet Pharmacol Ther* 2013;36:450–455.
- Leong RWL, Chang D, Merrett ND, et al. Taking optical biopsies with confocal endomicroscopy. *J Gastroenterol Hepatol* 2009;24:1701–1703.
- De Palma GD. Confocal laser endomicroscopy in the “*in vivo*” histological diagnosis of the gastrointestinal tract. *World J Gastroenterol* 2009;15:5770–5775.
- Dunbar KB, Kiesslich R, Deinert K, et al. Confocal laser endomicroscopy image interpretation: Interobserver agreement among gastroenterologists and pathologists. In: *Digestive Diseases Week – American Society for Gastrointestinal Endoscopy*. Washington, DC: Gastrointestinal Endoscopy; 2007: AB348.
- Nguyen NQ, Leong RWL. Current application of confocal endomicroscopy in gastrointestinal disorders. *J Gastroenterol Hepatol* 2008;23:1483–1491.
- Kitabatake S, Niwa Y, Miyahara R, et al. Confocal endomicroscopy for the diagnosis of gastric cancer *in vivo*. *Endoscopy* 2006;38:1110–1114.
- Watanabe O, Ando T, Maeda O, et al. Confocal endomicroscopy in patients with ulcerative colitis. *J Gastroenterol Hepatol* 2008;23:S286–S290.
- Leong RWL, Nguyen NQ, Meredith CG, et al. *In vivo* confocal endomicroscopy in the diagnosis and evaluation of celiac disease. *Gastroenterology* 2008;135:1870–1876.

14. Washabau RJ, Day MJ, Willard MD, et al. Endoscopic, biopsy, and histopathologic guidelines for the evaluation of gastrointestinal inflammation in companion animals. *J Vet Intern Med* 2010;24:10–26.
15. Willard MD, Moore GE, Denton BD, et al. Effect of tissue processing on assessment of endoscopic intestinal biopsies in dogs and cats. *J Vet Intern Med* 2010;24:84–89.
16. Dunbar K, Canto M. Confocal endomicroscopy. *Curr Opin Gastroenterol* 2008;24:631–637.
17. Boonacker E, Elferink S, Bardai A, et al. Fluorogenic substrate [Ala-Pro]2-cresyl violet but not Ala-Pro-rhodamine 110 is cleaved specifically by DPPIV activity: A study in living Jurkat cells and CD26/DPPIV-transfected Jurkat cells. *J Histochem Cytochem* 2003;51:969–968.
18. Tiffe HW, Matzke KH, Thiessen G. The acridine dyes: Their purification, physicochemical, and cytochemical properties. *Histochemistry* 1976;53:63–77.
19. Wirths K, Neuhaus H. Endomicroscopy of gastritis and gastric cancer. In: Kiesslich R, Galle PR, Neurath MF, eds. *Atlas of Endomicroscopy*. Heidelberg: Springer; 2008:60–66.
20. Trovato C, Sonzogni A, Ravizza D, et al. Celiac disease: In vivo diagnosis by confocal endomicroscopy. *Gastrointest Endosc* 2007;65:1096–1099.
21. Zhang JN, Li Y, Zhao YA, et al. Classification of gastric pit patterns by confocal endomicroscopy. *Gastrointest Endosc* 2008;67:843–853.
22. Moussata D, Goetz M, Gloeckner A, et al. Confocal laser endomicroscopy is a new imaging modality for recognition of intramucosal bacteria in inflammatory bowel disease in vivo. *Gut* 2011;60:26–33.
23. Goetz M, Kiesslich R, Neurath MF, et al. Functional and molecular imaging with confocal laser endomicroscopy. In: Kiesslich R, Galle PR, Neurath MF, eds. *Atlas of Endomicroscopy*. Heidelberg: Springer; 2008:87–92.
24. Moussata D, Goetz M, Watson AJ, et al. In vivo imaging of shedding cells induced by enteric bacteria using confocal endomicroscopy in humans. In: *Digestive Diseases Week – American Gastroenterological Association*. Chicago, IL: Gastroenterology; 2009:A130.
25. Watson AJ, Chu S, Sieck L, et al. Epithelial barrier function in vivo is sustained despite gaps in epithelial layers. *Gastroenterology* 2005;129:902–912.
26. Goetz M, Fottner C, Schirmacher E, et al. In vivo confocal real time mini-microscopy in animal models of human inflammatory and neoplastic diseases. *Endoscopy* 2007;39:350–356.
27. Aychek T, Vandoorne K, Brenner O, et al. Quantitative analysis of intravenously administered contrast media reveals changes in vascular barrier functions in a murine colitis model. *Magn Reson Med* 2011;66:235–243.
28. Vo LT, Papworth GD, Delaney PM, et al. In vivo mapping of the vascular changes in skin burns of anaesthetised mice by fibre optic confocal imaging (FOCI). *J Dermatol Sci* 2000;23:46–52.
29. Hughes OR, Ayling SM, Birchall MA. *In vivo* real time histology examination of the upper airway mucosa using confocal endomicroscopy. *Clin Otolaryngol* 2008;33:642.
30. Kiesslich R, Burg J, Vieth M, et al. Confocal laser endoscopy for diagnosing intraepithelial neoplasias and colorectal cancer in vivo. *Gastroenterology* 2004;127:706–713.
31. Buchner AM, Gomez V, Heckman MG, et al. The learning curve of in vivo probe-based confocal laser endomicroscopy for prediction of colorectal neoplasia. *Gastrointest Endosc* 2011;73:556–560.
32. Buchner AM, Shahid MW, Wallace AM. The learning curve of probe based CLE for detection of neoplasia in colon polyps. *Gastroenterology* 2010;138:S95.